



# Amniotic fluid mesenchymal stromal cells from early stages of embryonic development have higher self-renewal potential

JiETING HUANG<sup>1,2</sup> · WEI MA<sup>1</sup> · XIAOWEI WEI<sup>1</sup> · ZHENGWEI YUAN<sup>1</sup>

Received: 3 June 2020 / Accepted: 11 September 2020 / Published online: 7 October 2020 / Editor: Tetsuji Okamoto  
© The Society for In Vitro Biology 2020

## Abstract

Amniotic fluid (AF) is a rich source of mesenchymal stromal cells (MSCs) that have the ability to differentiate into multiple lineages rendering them a promising and powerful tool for regenerative medicine. However, information regarding the differences among AFMSCs derived from different gestational stages is limited. In the present study, AFMSCs derived from 125 pregnant rats at four embryonic day (E) stages (E12, E15, E18, and E21) were isolated and cultured. The primary E15 cells were the smallest in size and the easiest to culture and usually grew in a spherical shape that resembled the growth morphology of embryonic stem cells (ESCs). Once adhered, the E12 and E15 AFMSCs grew faster and could be passaged more than 60 times while still maintaining a continuous proliferative state; however, AFMSCs derived from E18 and E21 could normally be maintained for only 10 passages. To identify the possible reasons for this difference, RT-qPCR was used to examine several genes associated with self-renewal ability and cell origin. The Sox2 expression levels indicated that AFMSCs from E12 and E15 possessed stronger self-renewal capability. The K19, Col2A1, FGF5, AFP, and SPC expression levels indicated there were mixed-population cells co-existing in the AFMSC culture. In conclusion, E15 cells were easier to culture than E12 cells, could be passaged more often, and had a higher Sox2 expression than E18 or E21 cells. The E15-derived AFMSCs had higher viability and proliferative capacity than cells from the later stages. Therefore, AF cells from the early stages could be a good choice for exploring potential treatments involving AFMSCs.

**Keywords** Amniotic fluid · Embryonic development · Self-renewal potential · Cell size · Mesenchymal stromal cells

## Introduction

From the first discovery of the precursor cells, mechanocytes, 43 yr ago (Friedenstein 1976), to the naming of pluripotent progenitor cells in the embryo as mesenchymal stem cells (MSCs) 18 yr ago (Caplan 1991), to the first standard definition of multipotent MSCs by the International Society for Cellular Therapy 13 yr ago (Dominici *et al.* 2006), the field of MSC research has experienced numerous major advances, with basic research results currently

translated to clinical application. In several countries, MSCs have been used in phase III clinical trials to treat human diseases, such as graft versus host disease, heart disease, and Crohn's disease (Galipeau and Sensébé 2018). However, numerous differences exist in the MSCs obtained from different donors or different tissues, which influence the effects of MSCs as treatment. MSCs can be derived from numerous sources, such as bone marrow, adipose tissue, dental pulp, umbilical cord, amnion, amniotic fluid, and placenta. The most common source is bone marrow; however, bone marrow MSCs have certain limitations and sequential in vitro passages may lead to decreased proliferation and differentiation capacities and the appearance of senescence (Zheng *et al.* 2008). Therefore, identifying alternative multipotent cells is important. The Alessio team (Alessio *et al.* 2018) found amniotic fluid MSCs (AFMSCs) are less prone to senescence and more efficiently return to the basal condition after DNA damage compared with bone marrow MSCs. Furthermore, human first-trimester AF stem cells cultured in human embryonic stem cell (ESC) feeder-free culture medium share 82% of their transcriptome with ESCs

✉ Zhengwei Yuan  
yuanzw@hotmail.com

<sup>1</sup> Key Laboratory of Health Ministry for Congenital Malformation, Shengjing Hospital, China Medical University, No. 36, Sanhao Street, Heping District, Shenyang 110004, Liaoning, People's Republic of China

<sup>2</sup> BaYi Children's Hospital of the Seventh Medical Center of PLA General Hospital, Beijing 100700, People's Republic of China

(Moschidou *et al.* 2012). Bone marrow MSCs derived from younger donors are closer to ESCs than those from older donors (Billing *et al.* 2016). Thus, hypothetically, the closer the cells to the embryo source, the more similar their characteristics to ESCs.

The characteristics of AFMSCs are between somatic stem cells and ESCs (De Coppi *et al.* 2007). AFMSCs have self-renewal capacity, multilineage differentiation capability, lower immunogenicity, and, compared with ESCs, lower tumorigenicity (Spitzhorn *et al.* 2017). Their proliferation capability helps them expand and reach a large cell yield to meet clinical needs. Their homing specificity and proliferation rate allow AFMSCs to be used as vehicles for drug delivery, and their differentiation potential renders them useful for repairing damaged tissue and organs (Harrell *et al.* 2019). First-trimester AF stem cells can be reprogrammed to functional pluripotency in a similar manner to ESCs (Moschidou *et al.* 2012), and full-term AF stem cells exhibit high potency, similar to ESCs, spontaneously differentiating into the three germ layers and directly differentiating into neural lineage (Mun-Fun *et al.* 2015). Third-trimester AF stem cells harbor kidney progenitors (Rahman *et al.* 2018) and endothelial precursors (Schiavo *et al.* 2015). Third-trimester AF cells have better ability to repair a damaged carotid artery than cells from the second trimester (Schiavo *et al.* 2015). Third-trimester AFMSCs have lower potential for differentiation to myocytes and stronger potential for differentiation to neuron-like cells compared with second-trimester AFMSCs (Savickiene *et al.* 2015). The diverse morphologies of AFMSCs have different characteristics, with spindle-shaped AFMSCs demonstrating higher proliferation and differentiation than round-shaped cells (Rossi *et al.* 2014). In addition, discrepancies among the different numbers of AFMSC passages exist, with significant protein fluctuations observed at passages 5, 7, 11, and 25 and increased cell volume at passage 25, despite no changes in the karyotype, cell cycle, and apoptosis rate (Chen *et al.* 2009). Furthermore, AFMSCs from normal or fetal abnormality pregnancies also exhibited different senescence-associated characteristics (Savickienė *et al.* 2016). In brief, the focus in AFMSC studies was on cell diversity, whether derived from the first or second trimester, and research to identify the differences among AFMSCs over time throughout the pregnancy has not yet been conducted.

Accordingly, rat AFMSCs were compared from embryonic day 12 (E12) to E21, the basic biological phenomena at each stage recorded, and which cells had characteristics closer to ESCs determined. In contrast to E18 and E21 cells, AFMSCs isolated at E12 and E15 showed faster attachment to plastic culture plates at early cultivation, ESCs-like growth morphology, and higher renewal capacity. Conversely, the E18 and E21 cells stopped proliferating after 10 passages.

## Materials and Methods

**Animal preparation** Wistar rats were purchased from the animal center of China Medical University. All animal experiments were approved by the medical ethics committee of Shengjing Hospital of China Medical University, Shenyang, China (no. 2018PS108K). The AF cells were collected as early as possible to determine whether their characteristics were closer to ESCs at earlier stages and the sampling time points established to correspond to the stages of human pregnancy. Finally, E12, E15, E18, and E21 were chosen as the sampling time points because with our existing technique, the earliest gestational age at which cells can be isolated is E12. The E12, E15, E18, and E21 correspond to 1 mo, 2 mo, 6 mo, and full-term human pregnancy (Hill 2019), which is equivalent to early (E12, E15), middle (E18), and late pregnancy (E21).

Samples were taken from the vaginas of female rats after they mated with male rats, spread on a coverslip using a cotton swab, and examined; if sperm was observed, day 0 of pregnancy (E0) was recorded. Subsequently, at E12, E15, E18, and E21, the female rats were sacrificed by injection with an overdose of 10% chloral hydrate via the peritoneum, and the uteri were isolated and transferred to a sterilized Petri dish and placed on ice. The uteri were rinsed three times with sterilized saline and then opened to isolate the amniotic sac. AF was carefully aspirated using a 1-mL sterilized syringe and transferred to centrifuge tubes for further processing.

**Primary cell culture** The cells were isolated according to the previously published protocol (Kaviani *et al.* 2001; Li *et al.* 2014; Lesage *et al.* 2017). Briefly, the collected AF was centrifuged immediately at 1800 rpm at 4°C for 15 min, the supernatant was carefully removed and discarded, and the cell pellet was washed three times with sterilized  $1 \times$  PBS. The AF cell pellets were then resuspended in 1 mL of DMEM/F12 (Biological Industries, Shanghai, China) supplemented with 10% FBS (Corning Inc., Corning, NY) and placed in a well of a 24-well culture plate or 12-/6-well culture plate (Thermo Fisher Scientific, Wilmington, DE) at a cell density of approximately  $1.0\text{--}1.5 \times 10^5/\text{cm}^2$ . The cells were then maintained in a 5% CO<sub>2</sub> incubator at 37°C. The cells were observed everyday under an inverted microscope; if the cell morphology changed significantly, a photomicrograph was taken. The medium was first replaced on the 5th day after seeding and then every 1 or 2 d. When 70–80% confluence was reached, the cells were detached by treatment with 0.25% trypsin/EDTA (Gibco, Grand Island, NY) for 1 min after washing with  $1 \times$  PBS, trypsin activity was inhibited by the addition of an appropriate amount of fresh DMEM/F12 medium, and the cells in the suspension were then passaged onto a plate or flask at a cell density of  $3.5\text{--}5.0 \times 10^4/\text{cm}^2$ . Subsequently, every 3 or 4 d, the AFMSCs in each group were split to a new flask at a ratio of 1:2 or 1:3 when they reached 90% confluence. Cells

that were maintained and subcultured under these conditions for three passages (P3) were defined as a successful culture. All cells used in this study comprised at least three independent samples for each gestational age and were randomly selected, unless stated otherwise.

**Cell counting** At each stage of the cell isolation and culture, the number of cells was determined using a cell counter (Countess<sup>TM</sup> II Automated Cell Counter, Invitrogen, Carlsbad, CA, Thermo Fisher Scientific), which automatically records various characteristics, such as cell size, total concentration, and viability. The cell size and number in each group were used for subsequent statistical analysis.

**Immunophenotypic characterization based on flow cytometry** Appropriately subcultured AF cells at P4 were briefly washed with  $1 \times$  PBS and detached from the flasks by treatment with trypsin. The cells were then resuspended in  $100 \mu\text{L}$   $1 \times$  PBS containing  $1 \mu\text{L}$  fluorochrome-conjugated monoclonal antibodies CD29-FITC and CD90-PE (cat no. 561796 and 551401, respectively; BD Biosciences, San Jose, CA) and  $5 \mu\text{L}$  CD45-FITC and CD34-FITC (cat no. sc1187 and sc7324, respectively; Santa Cruz Biotechnology, Santa Cruz, CA) for staining. The cells were incubated for 30 min at  $4^\circ\text{C}$  in the dark and then rinsed with  $1 \times$  PBS and resuspended in  $400 \mu\text{L}$  of  $1 \times$  PBS solution before being quantified using a Beckman Coulter CytoFLEX flow cytometry system set to detect CD surface markers.

**In vitro differentiation of AFMSCs** The Wistar Rat Mesenchymal Stem Cell Chondrogenic Differentiation Medium Kit (cat. no. RAWMX-90042; Cyagen, Santa Clara, CA) was used for the chondrogenic differentiation. According to the manufacturer's instructions, the four groups of AFMSCs at P5 were resuspended in 1 mL Incomplete Chondrogenic Medium per  $7.5 \times 10^5$  cells and centrifuged at 150g for 5 min. The medium was then discarded and the AFMSCs were resuspended in Complete Chondrogenic Medium to a concentration of  $5.0 \times 10^5$  cells/mL. Next, 0.5 mL ( $2.5 \times 10^5$  cells) of the cell suspension was aliquoted into 15-mL polypropylene culture tubes and the cells were centrifuged at 150g for 5 min at room temperature and maintained in a 5%  $\text{CO}_2$  incubator at  $37^\circ\text{C}$ . The medium was replaced every 2–3 d; at 21 d, chondrogenic pellets were successfully induced. The pellets were fixed in 10% formalin, paraffin embedded, sectioned, and stained with Alcian blue.

The Wistar Rat Mesenchymal Stem Cell Adipogenic Differentiation Medium Kit (cat no. RAWMX-90031; Cyagen) was used for adipogenic differentiation. According to the manufacturer's instructions,  $1 \times 10^6$  cells at P5 were seeded onto 6-well plates (Corning Inc.) and incubated overnight in DMEM/F12 (BI) medium supplemented with 10% FBS (Corning Inc.). The medium was then changed to

differentiation medium A for 3 d, to differentiation medium B for 1 d, and to medium A for 3 d. After four such cycles, the cultures were maintained in medium B for 3 d. The differentiation potential for adipose cells was assessed using Oil Red O staining.

The Wistar Rat Mesenchymal Stem Cell Osteogenic Differentiation Medium Kit (cat no. RAWMX-90021, Cyagen) was used for osteogenic differentiation. As instructed,  $5 \times 10^5$  cells at P5 were seeded onto 0.1% gelatin-coated 6-well plates (Corning Inc.) and incubated overnight in DMEM/F12 (BI) medium supplemented with 10% FBS (Corning Inc.). The medium was then changed to the differentiation medium for 21 d. The differentiation medium was replaced every 3 d. To determine osteogenic differentiation, calcium deposits were monitored using Alizarin Red staining.

**Colony-forming unit-fibroblast assay** When AFMSCs at P4 reached 90% confluence, they were detached and seeded onto 6-well plates at a density of 100 cells/well. After 14 d of culture, the cells were fixed using methanol for 30 min and stained with crystal violet staining solution (Biotime, Jiangsu, P.R., China) for 20 min. The colony-forming unit-fibroblast (CFU-F) number was scored microscopically by counting colonies ( $\geq 50$  cells) with clear spindle-shaped fibroblast-like morphology and excluding colonies with round-shape epithelioid-like morphology.

**BrdU test** An APC BrdU Flow Kit (cat. no. 552598, BD Biosciences) was used for the BrdU experiments. E18 and E21 AFMSCs at P11 and E12 and E15 AFMSCs at P50 were labeled with BrdU solution for 4 h in a 5%  $\text{CO}_2$  incubator at  $37^\circ\text{C}$ . The cells were then resuspended and incubated in  $100 \mu\text{L}$  of BD Cytofix/Cytoperm Buffer for 20 min at room temperature and treated with  $100 \mu\text{L}$  of BD Cytoperm Permeabilization Buffer Plus for 10 min on ice. The cells were re-fixed with  $100 \mu\text{L}$  of BD Cytofix/Cytoperm Buffer for 5 min at room temperature and then treated with  $100 \mu\text{L}$  of DNase for 1 h at  $37^\circ\text{C}$ . Finally, the cells were incubated with  $50 \mu\text{L}$  of the APC anti-BrdU antibody (1:50 dilution) for 20 min at room temperature in the dark and then with  $20 \mu\text{L}$  of the 7-AAD solution for another 20 min. A Beckman Coulter CytoFLEX flow cytometry was used to analyze the differences in the S-stage ratios of the four groups of AFMSCs.

**RNA extraction and RT-qPCR** From AFMSCs derived from the four stages of rat pregnancy, three to four samples at each gestational age were randomly selected and used for RNA extraction and RT-qPCR, resulting in 24–36 RNA samples: 12 samples of primary cells and 12–16 samples of P4 cells. The primary cells and P4 AFMSCs were harvested as described above. After being rinsed with  $1 \times$  PBS, cell pellets

were resuspended and lysed in 1 mL of TRIzol RNA extraction reagent (Ambion, Foster City, CA) and incubated on ice for 10 min. The mass of RNA and protein was separated by the addition of trichloromethane. The top layer of the solution, which contained the RNA, was removed and transferred to a fresh tube and the RNA was precipitated by the addition of an appropriate amount of cold isopropanol. At the end, 1 mL of ethanol was added to purify the RNA. The RNA was dissolved in 20  $\mu$ L of RNase-free water and its concentration quantified using a NanoDrop 2000 spectrophotometer (Thermo Fisher Scientific). The reverse transcription reactions were performed using a Takara PrimeScript RT Reagent Kit according to the manufacturer's instructions (Takara Bio, Inc., Shiga, Japan). TB Green<sup>TM</sup> Premix Ex Taq<sup>TM</sup> II (Takara Bio Inc.) was used for the RT-qPCR. The following conditions were used for the reaction: 45 cycles of pre-denaturation at 95°C for 30 s, 95°C for 5 s, and 60°C for 34 s for the PCR reaction, followed by 95°C for 5 s and 60°C for 30 s for the last dissolution stage. An ABS 7500 PCR System (Applied Biosystems, Carlsbad, CA) was used to detect the following genes: Sox2, Oct4, Nanog, AFP, FGF5, SPC, K19, and Col2A1. Sox2, Oct4, and Nanog were analyzed as stemness markers (Savickiene *et al.* 2015) and AFP, FGF5, SPC, K19, and Col2A1 as markers of fetal endoderm, neuroderm, respiratory tract, skin, and cartilage, respectively (Akagi *et al.* 2015; Hoepfner *et al.* 2016; Honarpardaz *et al.* 2019; Irfan-Maqsood *et al.* 2016; Jensen *et al.* 2017).  $\beta$ -actin was used as the internal control as follows:  $\Delta$ CT (cycle threshold) =  $CT_{\text{target}} - CT_{\text{internal control}}$ . At least three samples from each stage of AFMSCs were used in the PCR, and each test was repeated twice. The relative expression levels of the target genes were calculated as follows:  $2^{-\Delta\Delta CT}$ , with the  $\Delta\Delta CT$  equal to  $\Delta CT_{E12, E18 \text{ or } E21} - \Delta CT_{E15}$ . The forward and reverse primers are shown in Table 1.

**Immunofluorescence** Anti-collagen II antibody (COL2A1, ab34712, Abcam, Cambridge, UK), cytokeratin 19 (K19, sc-376126, Santa Cruz Biotechnology), and SFTPC antibody (SPC, 10774-1-AP, Proteintech, Chicago, IL) were applied according to the manufacturers' protocols. The four groups of AFMSCs at P5 were seeded overnight on 24-well coverslips (WHB-24-CS, WHB, Shanghai, China). The coverslips were rinsed with 1  $\times$  PBS twice the next day, fixed with methanol for 30 min, and then rinsed with 1  $\times$  PBS three times again. PBS containing 10% FBS and 0.1% Triton X-100 was used to block non-specific antigen binding for 30 min and then the cells were incubated with primary antibodies for 2 h at room temperature. The secondary antibodies anti-rabbit IgG (Alexa Fluor® 488 Conjugate) and anti-mouse IgG (Alexa Fluor® 555 Conjugate) (4412 and 4409, Cell Signaling Technology, Inc., Beverly, MA) were used at 1:100 dilution for another 2 h at room temperature. DAPI

**Table 1.** Primer sequences of the specific genes used in RT-qPCR to identify the origins of the fetal tissues

Gene	Direction	Primer sequence (5'-3')
$\beta$ -actin	Forward	GGAGATTACTGCCCTGGCTCCTA
	Reverse	GACTCATCGTACTCCTGCTTGCTG
Sox2	Forward	CGGCGGCAACCAGAAGAACAG
	Reverse	CGCTTGGCCTCGTCGATGAAC
Nanog	Forward	ATGCCTGCCGTTTCATCTTC
	Reverse	GGACCTTGTCTCTCTCTTTC TTCTC
AFP	Forward	ACTGGCGATGGGTGTTTAGA
	Reverse	AGTCTGGAGCGGTCTTCTTG
FGF5	Forward	CGACGTTTGCTTCGCTCTTCT
	Reverse	ACTTTGCCATCCGGGTAGAT
SPC	Forward	TCGTGGTTGTGGTGGTAG
	Reverse	GAAGGTAGCGATGGTGTCT
K19	Forward	TCAGTCTTGCGGTTGAAGTG
	Reverse	AAAGGGAAGCCGAATCACA
Col2A1	Forward	ACGCTCAAGTCGCTGAACAACC
	Reverse	AGGCTCACCGCTCTTCCACTC
Oct4	Forward	TGGAATCGGACCAGGTTTCAGAGG
	Reverse	GCAGAGTCTCCACGCCAACTTG

staining was performed and the cells were observed under a fluorescence microscope (E2000S, Olympus, Shinjuko, Tokyo, Japan).

**Statistical analysis** The surface markers, CFU-F assay, and RT-qPCR experiments described in this study were biologically repeated at least three times. The results are recorded as mean  $\pm$  standard deviation of the mean and were analyzed using Kruskal-Wallis (AF volumes, AF cell densities, and immunofluorescence) or one-way ANOVA (cell areas, the time of the first clone appearance, RT-qPCR data, BrdU, and CFU-F assays). Post hoc analysis was used for the LSD or the Tamhane T2 using the SPSS 23.0 software. A  $p$  value < 0.05 was considered to indicate a statistically significant difference between sets of data.

## Results

**Heterogeneity of AFMSCs derived from different rat gestational ages** We collected AF from 125 pregnant female rats at four different stages of pregnancy as described above and used it for primary cell culture and isolation of AFMSCs. Of the various cultures, 47 were derived from E12, 17 from E15, 44 from E18, and 17 from E21 (Table 2). Only those cultures that survived three passages were considered a success and included in these analyses (Table 2). The cultures derived

**Table 2.** Success rates (survived three passages) of the primary cultures of AF cells derived from the different gestational stages of pregnant rats

	E12	E15	E18	E21
AF isolation	47	17	44	17
Culture success	9 (19.15%)	17 (100%)	15 (34.09%)	11 (64.71%)

from the E15 stage had a 100% success rate, and the cultures derived from the E12, E18, and E21 stage had 19.15%, 34.09%, and 64.71% success rates, respectively, under the same culture conditions. The imaging software ImageJ was used to calculate the cell areas of the four stages of AFMSCs at P4 (Fig. 1e–h,  $\times 100$  magnification, 30 cells at random). The mean areas were  $1156.76 \pm 274.72 \mu\text{m}^2$ ,  $989.11 \pm 348.67 \mu\text{m}^2$ ,  $3580.82 \pm 1006.9 \mu\text{m}^2$ , and  $6188.67 \pm 3263.86 \mu\text{m}^2$  for E12, E15, E18, and E21, respectively (Fig. 1a), which indicates the E15 cells were the smallest. In addition, the

original density of the AF cells gradually decreased before E18 and then increased again at the full-term (E21) stage (Fig. 1b) due to the changes in the total volumes of the AFs at the different stages (Fig. 1c). The data indicate that there was no correlation between the cell culture success rate and the original density of the AF cells derived from the different stages of pregnancy under the current experimental conditions.

After the AF cells were seeded in a culture plate, fibroblast-like cells were observed at days 1–3 from E12 and E15 cells but could only be observed for the other gestational ages at approximately days 5–7 or later (Fig. 1i–l). The exact time of the first clone appearance was  $2.11 \pm 1.05$  d for E12 AFMSCs,  $1.47 \pm 0.8$  d for E15,  $5.53 \pm 1.51$  d for E18, and  $6.36 \pm 1.43$  d for E21. Significant differences were observed among the E12, E15, E18, and E21 cells (Fig. 1d). In addition, the morphologies of the adhered cells differed. The cells derived from E12 and E15 AF, particularly E15, tended to cluster in a spherical shape, which was similar to the morphology of

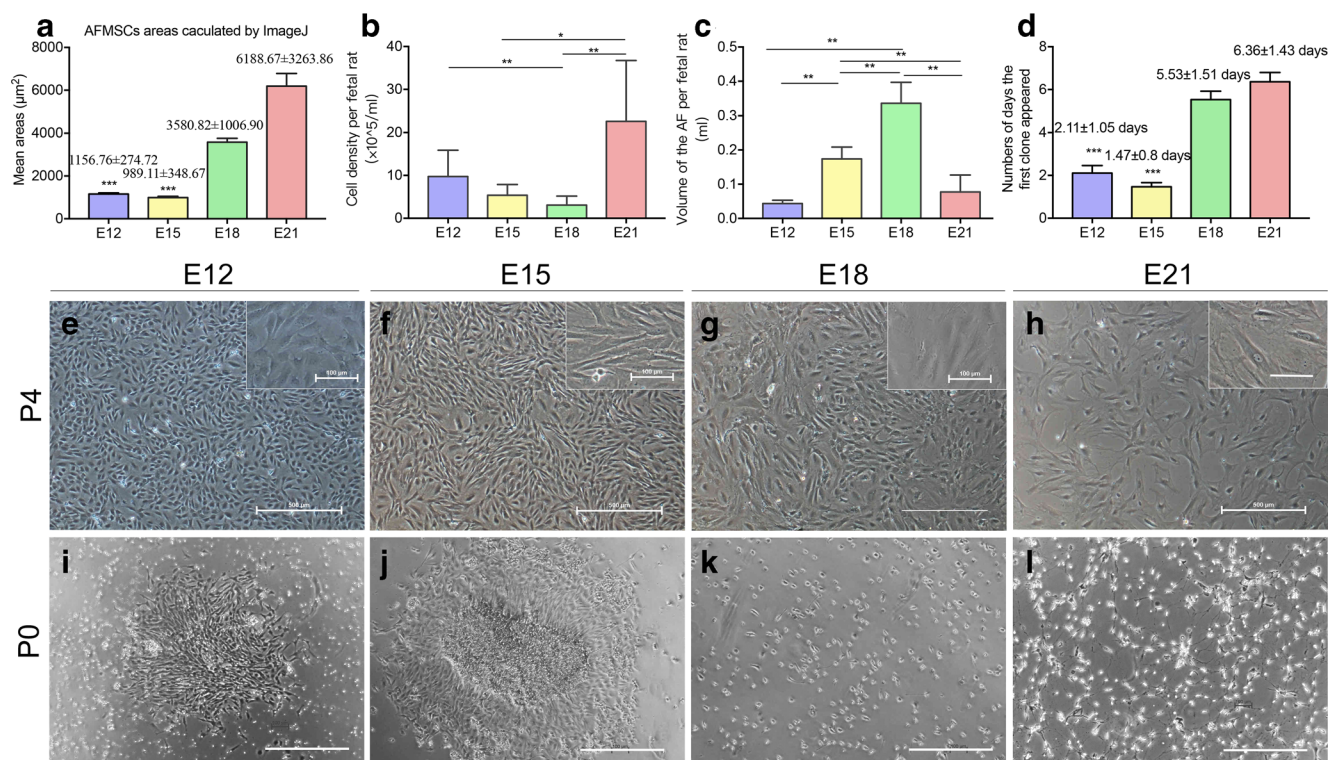


**Figure 1.** Cell size, density, and morphological characteristics of MSCs derived from rat AF at different stages of embryonic development. (a) Mean areas of the four stages of AFMSCs at P4 (using the magnified images in Fig. 1e–h) calculated from 30 randomly selected cells. The cells derived from E15 were among the smallest (ANOVA,  $F$  value = 60.502,  $p < 0.001$ ); within the groups, the  $p$  values were 0.233,  $< 0.001$ , and  $< 0.001$  for E12, E18, and E21 compared with E15, respectively. (b) AF cell density at the different gestational ages; the difference was significant (Kruskal-Wallis test, chi-squared = 21.730,  $p < 0.001$ ). (c) AF volumes at the different gestational ages; the difference was significant (Kruskal-Wallis test, chi-squared = 60.744,  $p < 0.001$ ). (d) The timing of the first clone appearance (ANOVA,  $F$  value = 52.719,  $p < 0.01$ ); within the

groups, the  $p$  values were 0.209,  $< 0.001$ , and  $< 0.001$  for E12, E18, and E21 compared with E15, respectively. For b, the number of samples was  $n_{E12} = 20$ ,  $n_{E15} = 9$ ,  $n_{E18} = 19$ , and  $n_{E21} = 9$ . For c, the number of samples was  $n_{E12} = 32$ ,  $n_{E15} = 11$ ,  $n_{E18} = 23$ , and  $n_{E21} = 10$ . For d, the sample replicate number was  $n_{E12} = 9$ ,  $n_{E15} = 17$ ,  $n_{E18} = 15$ , and  $n_{E21} = 11$ . (e–h) AFMSCs at P4 show the typical fibroblast-like cell morphology and adherence to plastic plates. Scale bar = 500  $\mu\text{m}$ . The photomicrograph in the upper right corner is a magnified image of the cells. Scale bar = 100  $\mu\text{m}$ . (i–l) AFMSCs at P0 show compact clones in E12 and E15 AFMSCs within 3 d compared with the E18 and E21 AFMSCs, which show no clone growth. Scale bar = 500  $\mu\text{m}$ , \* $p < 0.05$ , \*\* $p < 0.01$ , and \*\*\* $p < 0.001$  compared with E18 and E21.

ESCs. In contrast, the cells derived from the E18 and E21 AF grew scattered around the plates. After being subcultured to P4, AFMSCs derived from the E18 and E21 AF adopted a larger and rounder shape (Fig. 1e–h).

To explore the proliferation potential of the AFMSCs derived from the four different stages, cells were randomly selected for long-time culture observation. Five samples of E12 and E15 AFMSCs were used to investigate the growth potential; all could be maintained to P60. In contrast, although 44 samples of E18 and 17 samples of E21 AFMSCs were used to investigate the growth potential, most could not be grown to P7 and only 3 of the 17 E21 AFMSCs and 2 of the 44 E18 AFMSCs could be passaged beyond P10. Thus, the mean passage number of both E12 and E15 AFMSCs was 60 and reached  $2.306 \times 10^{24}$  cells; E18 AFMSCs reached  $1.344 \pm 1.761 \times 10^8$  and E21 AFMSCs reached  $3.087 \pm 0.9631 \times 10^8$  (Table 3). In addition, a BrdU test was performed to confirm whether the cells would continue growing. The E12 and E15 cells at P50 had a higher S-stage ratio than the E18 and E21 cells at P11 (Fig. 2). This result indicates that AFMSCs derived from early gestational ages maintained the state of cell division until P50 but the cells derived from E18 and E21 could not maintain the state of cell division after P11.

**AFMSC identification at the different stages** As described above, the four groups of cells were stained with both MSC-positive (CD29 and CD90) and MSC-negative (CD34 and CD45) markers and then analyzed using flow cytometry. The results showed that all cells displayed a similar positive expression of CD90 and CD29 and lacked expression of CD34 and CD45 (Fig. 3). In accordance with the trilineage differentiation, all groups of cells could be marked with Alcian blue staining for chondrogenic differentiation, Oil Red O staining for adipogenic differentiation, and Alizarin Red staining for osteogenic differentiation (Fig. 4a–o), showing these cells meet the criteria of AFMSCs. In addition, the chondrogenic and adipogenic differentiation was not significantly different (Fig. 4p–q) and the E12 and E15 AFMSCs had higher osteogenic differentiation capacity (Fig. 4r).

**AFMSCs derived from E12 and E15 AF possess stronger proliferative capability** Because the morphology of the AFMSCs derived from E12 and E15 resembled ESCs, we hypothesized these cells would possess stronger stemness. To test this

theory, a CFU-F assay was performed and the expression of Sox2, Oct4, and Nanog genes was examined using RT-qPCR. These genes were chosen because they are regarded as typical stemness markers (Savickiene *et al.* 2015). The CFU-F assay results indicated that E12 and E15 AFMSCs had greater capacity for clone generation than E18 and E21 AFMSCs (Fig. 5a–b). The RT-qPCR results showed that except for E21 AFMSCs, all AFMSCs expressed Oct4, and all four groups of AFMSCs expressed Sox2 (Fig. 5c) but did not express Nanog. The Oct4 expression was not significant among the groups; however, the Sox2 expression was significantly higher for early-stage AFMSCs than later stages. Thus, the results support the hypothesis that AFMSCs are similar to but not the same as ESCs (Pratheesh *et al.* 2013) and AFMSCs derived from the earlier stages of pregnancy possess stronger proliferative capability than those from later stages.

**AFMSCs are mixed-population cells** Whether the variations in the morphology and the proliferative potency of AFMSCs at the four gestational ages correlated with the original sources of the fetal tissues was investigated. RT-qPCR was used to examine the expression of K19, a fetal skin marker (Irfan-Maqsood *et al.* 2016), AFP, an endoderm marker (Hoepfner *et al.* 2016), FGF5, an ectoderm marker (Akagi *et al.* 2015), SPC, a respiratory tract marker (Jensen *et al.* 2017), and Col2A1, a cartilage marker (Honarpardaz *et al.* 2019) in all four groups of primary AF cells and AFMSCs at P4. In the primary AF cells, the K19 gene expression was obvious at all four gestational stages; however, the Col2A1 and AFP gene expressions were obvious only at early gestational stages (Fig. 5d). K19, Col2A1, FGF5, and AFP genes were expressed in all AFMSCs at P4; however, the SPC gene was expressed only in E18 and E21 AFMSCs (Fig. 5e). In addition, immunofluorescence of COL2A1, K19, and SPC was performed; the results supported the PCR results (Figs. 6 and 7). In summary, the E12 AFMSCs expressed K19, Col2A1, FGF5, and AFP genes, indicating these AFMSCs were from fetal skin, cartilage, ectoderm, and endoderm, respectively. The E15 AFMSCs mainly expressed K19, Col2A1, and FGF5, indicating these AFMSCs were from fetal skin, cartilage, and ectoderm, respectively. The main genes expressed in the E18 AFMSCs were K19, Col2A1, FGF5, and SPC, indicating that fetal skin, cartilage, ectoderm, and respiratory tract, respectively, were the origin of the AFMSCs at the E18 stage. The

**Table 3.** The proliferation potentials of the four AFMSCs derived from the different stages

	E12	E15	E18	E21
The numbers of observed samples	5	5	44	17
Mean passages (mean (SD))	60	60	6.07 (6.46)	7.27 (5.59)
Mean numbers of AFMSCs	$2.306 \times 10^{24}$	$2.306 \times 10^{24}$	$(1.344 \pm 1.761) \times 10^8$	$(3.087 \pm 0.9631) \times 10^8$

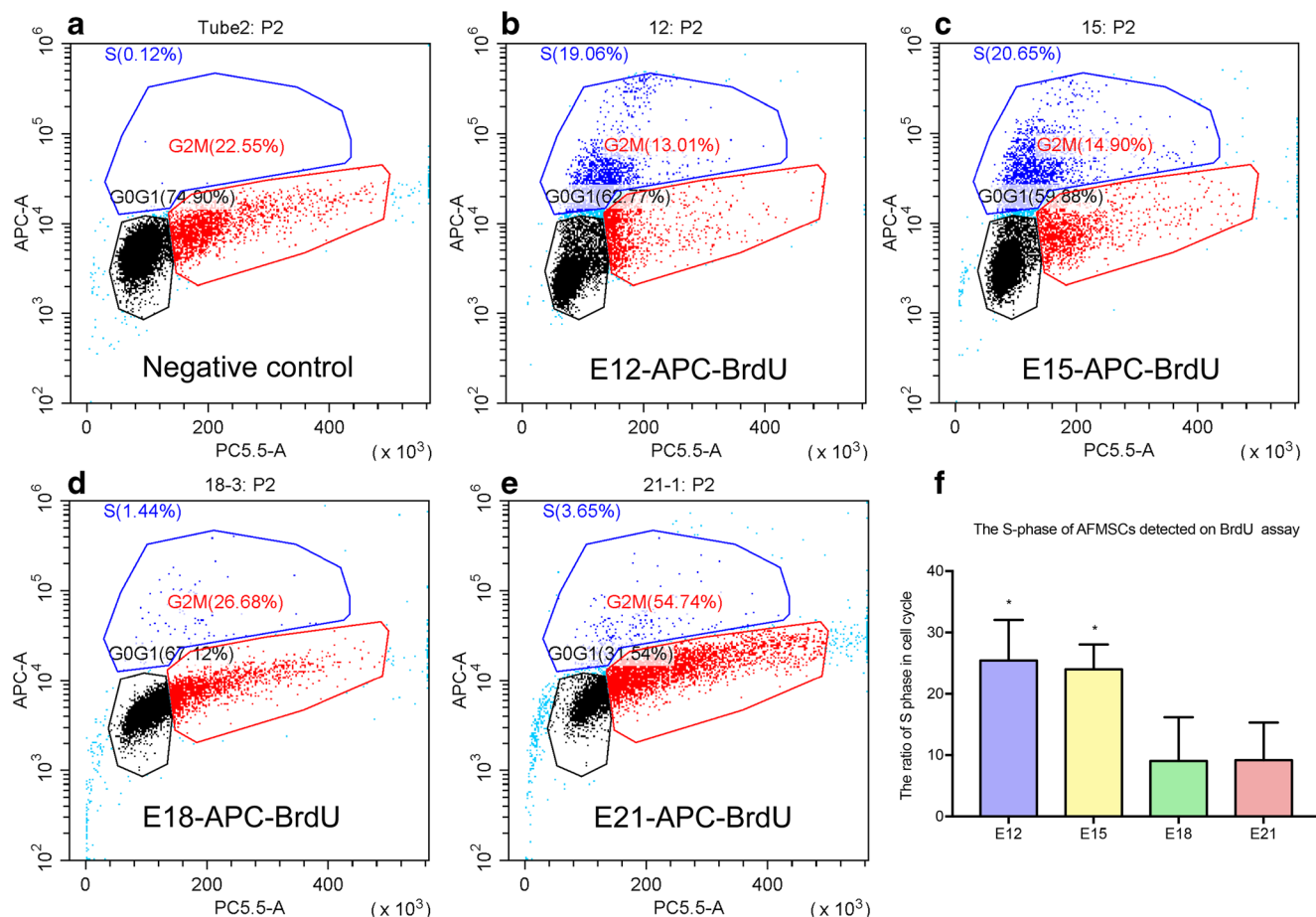


**Figure 2.** BrdU detected using flow cytometry in AFMSCs. (a) APC negative control of AFMSCs. (b) Among E12 AFMSCs at P50, 19.06% were stained with APC anti-BrdU. (c) Among E15 AFMSCs at P50, 20.65% were stained with APC anti-BrdU. (d) Among E18

AFMSCs at P11, 1.44% were stained with APC anti-BrdU. (e) Among E21 AFMSCs at P11, 3.65% were stained with APC anti-BrdU. (f) The mean S-phase ratio in the four groups of AFMSCs.  $n = 3$ ,  $F = 6.66$ ,  $p = 0.014$ ,  $*p < 0.05$  compared with E18 and E21.

main genes expressed in the E21 AFMSCs were K19, Col2A1, and FGF5, indicating the E21 AFMSCs originated from fetal skin, cartilage, and ectoderm, respectively.

## Discussion

The composition of AF is maintained in a dynamic equilibrium throughout pregnancy and differs at different gestational ages. In humans, the early AF is mainly composed of maternal serum that enters the amniotic cavity through the amniotic membrane, as well as a small amount of water and a small number of molecular substances discharged from the early fetal skin (Underwood *et al.* 2005). In the middle trimester of pregnancy, although the materials discharged from the skin gradually disappear, fetal urine appears, and the fetus begins to swallow some of the AF. By the late trimester, the AF is mainly composed of fetal urine, some discharged substances that are partly excreted from the fetal lungs, various small

molecular substances, and liquid that is exchanged through the placenta.

Because the AF differs at each stage of pregnancy, the types of cells that are present also change. Studies of the differences among AFMSCs have mainly focused on various cellular morphologies (Roubelakis *et al.* 2011; Rossi *et al.* 2014) or the functional differences among different passages (Chen *et al.* 2009) but lacked any comparison of cells sequentially derived from different periods of pregnancy, except in Rahman *et al.* (2018) and Rossi *et al.* (2014). However, Rahman *et al.* compared human AFMSCs of three trimesters and focused on the effects of different culture media and the expression trends of genes of renal origin. Rossi's team focused on the diversity of various cellular morphologies. The differences among AFMSCs derived from sequential gestational ages remain unclear.

In the present study, AF cells were isolated from the AF of pregnant rats at E12, E15, E18, and E21. Because the data indicated that most cells harvested at P4 were positive for CD29 and CD90 but negative for CD34 and CD45 (Fig. 3),

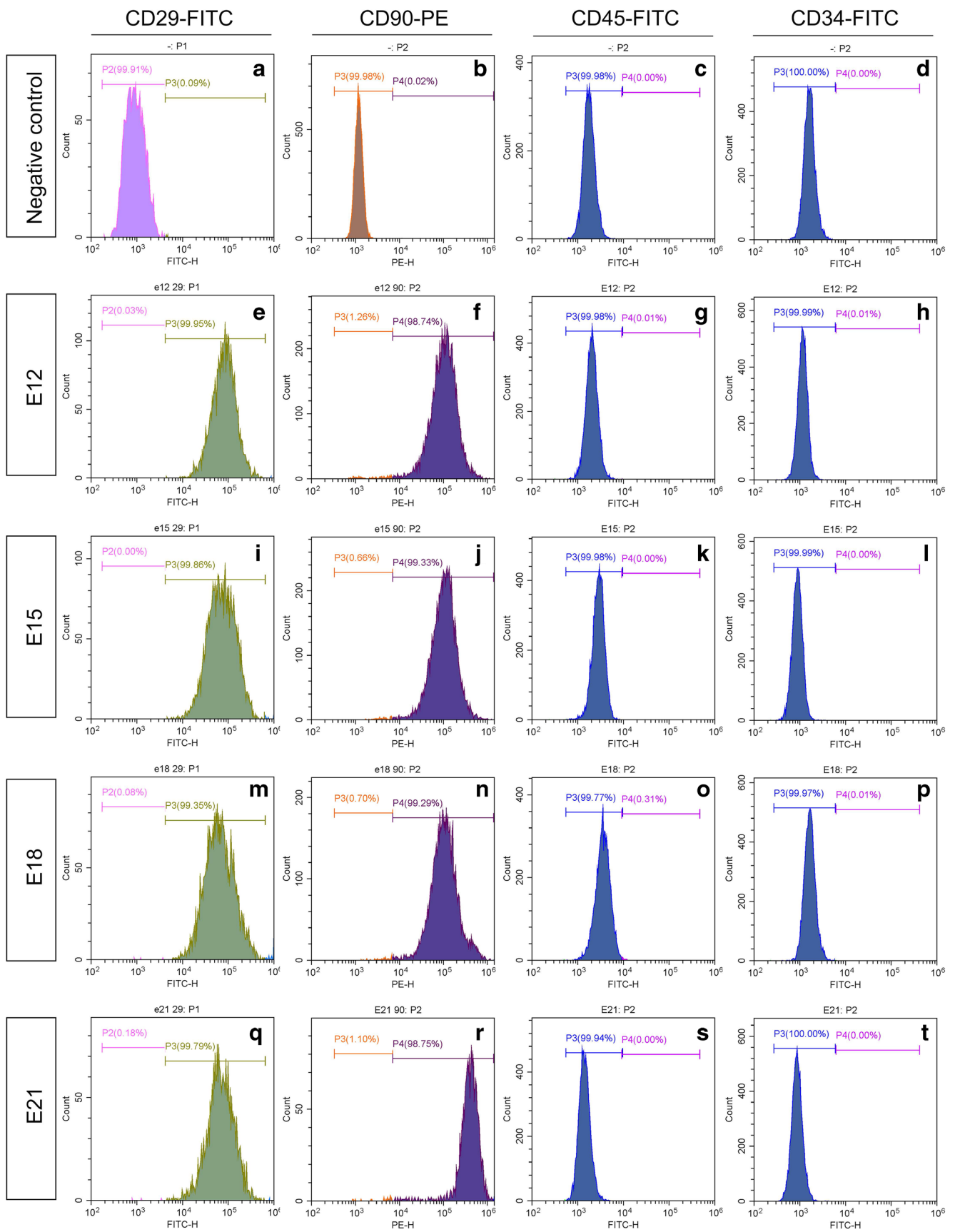


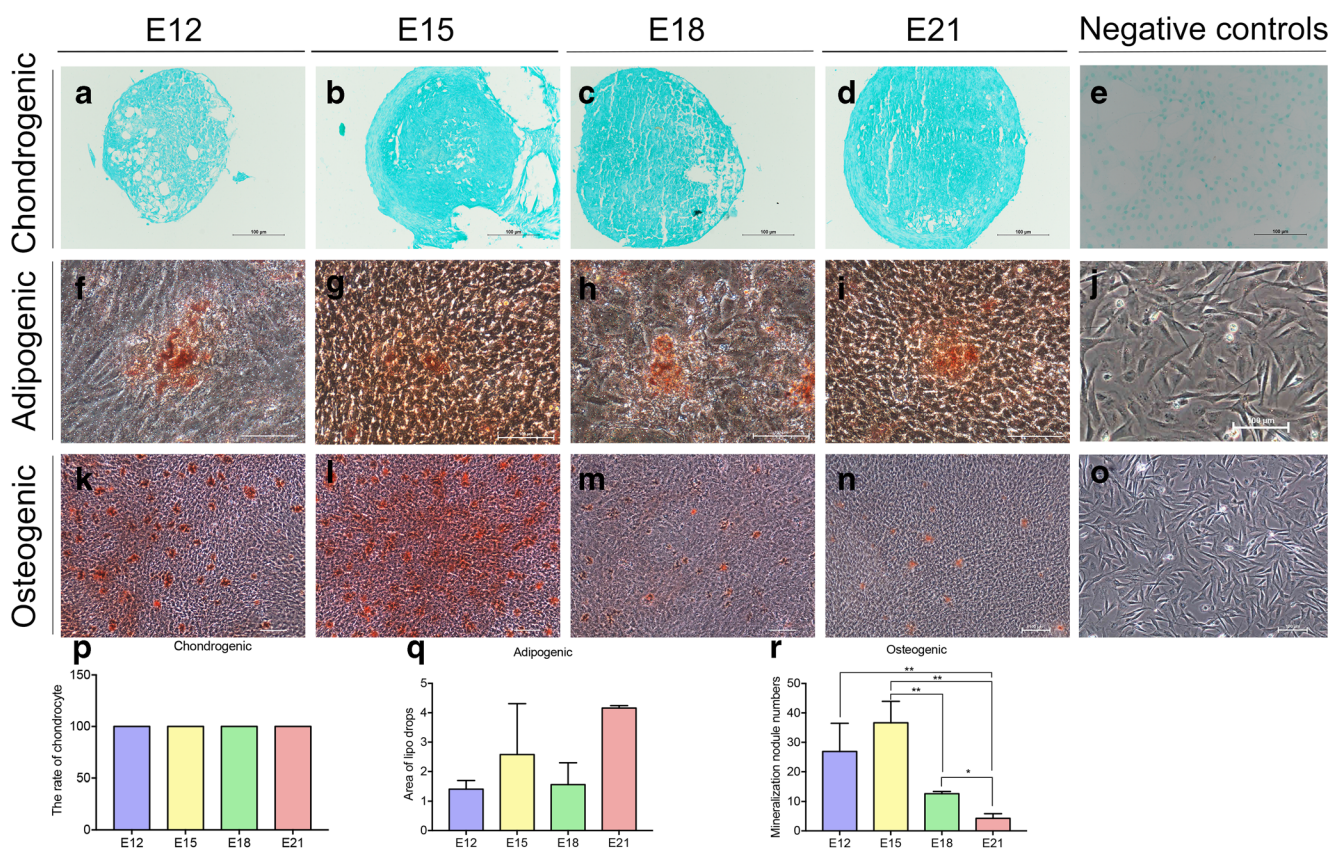


**Figure 3.** MSC surface markers detected using flow cytometry in P4 AFMSCs derived from four stages of pregnant rats. (a–d) The negative control of CD29-FITC, CD90-PE, CD45-FITC and CD34-FITC, respectively. (e–h) Surface marker expression of AFMSCs derived from E12. (i–l) Surface marker expression of AFMSCs derived from E15. m–p Surface marker expression of AFMSCs derived from E18. (q–t) Surface marker expression of AFMSCs derived from E21.  $n = 3$ .

had trilineage differentiation capacity, and adhered to plastic labware, the cells were considered to be AFMSCs. The cells from E15 had the highest rate of successful culture; however, the cells from E12 were the most difficult to culture. We hypothesized the rat uteri at E12 had less AF; thus, fewer cells were collected (Fig. 1b–c) and their extracellular secretions cannot create the stable microenvironment that supports cell growth (Dostert *et al.* 2017) or meet the *in vitro* expanded basic condition, leading to the extremely low success rate of cultured AFMSCs. After E15, fetal tissue and organs gradually matured and the stem cells with high proliferation potency decreased, resulting in lower culture success rate at E18 and E21. In addition, the cells derived from the E15 stage had the smallest cell size. The higher the ratio of small cells, the higher the proliferative capacity and the higher the self-renewal

capacity (Samsonraj *et al.* 2015), which may be another reason why E15 AFMSCs were the easiest to culture.

AFMSCs derived from the four distinct stages, E12, E15, E18, and E21, displayed significantly distinct growing behavior. The cells derived from E12 and E15 AF formed dense fibroblast-like and clustered spherical colonies as early as 1–3 d after seeding, which resembled ESC growth (Pratheesh *et al.* 2013). In the E18 and E21 samples, growth only occurred after 5–7 d in culture and the cells were scattered around the plates. Moschidou *et al.* (2012) showed that AF cells derived from first-trimester AF in humans can grow in a spherical shape and behave in a similar manner to ESCs, which is consistent with our observations in rats. Therefore, cells derived from E12 and E15 AF potentially possess stronger stemness characteristics than cells derived from E18 and E21. The present study results showed the Sox2 expression was significantly increased in the cells from E12 and E15. Sox2 is an important regulatory factor for maintaining pluripotent stem cells; the higher Sox2 expression indicated the cells from E12 and E15 have higher self-renewal potential. In addition, the Oct4 expression was not significantly higher at E12 and E15. Oct4



is the negative control. Scale bar = 100  $\mu$ m. (p) The statistical histogram of chondrogenic differentiation. (q) The statistical histogram of adipogenic differentiation did not show significant difference; Kruskal-Wallis test, chi-squared = 6.436,  $n = 3$ . (r) The statistical histogram of osteogenic differentiation; Kruskal-Wallis test, chi-squared = 24.03,  $n = 8$ ,  $*p < 0.05$ ;  $**p < 0.01$ .

is the negative control. Scale bar = 100  $\mu$ m. (p) The statistical histogram of chondrogenic differentiation. (q) The statistical histogram of adipogenic differentiation did not show significant difference; Kruskal-Wallis test, chi-squared = 6.436,  $n = 3$ . (r) The statistical histogram of osteogenic differentiation; Kruskal-Wallis test, chi-squared = 24.03,  $n = 8$ ,  $*p < 0.05$ ;  $**p < 0.01$ .

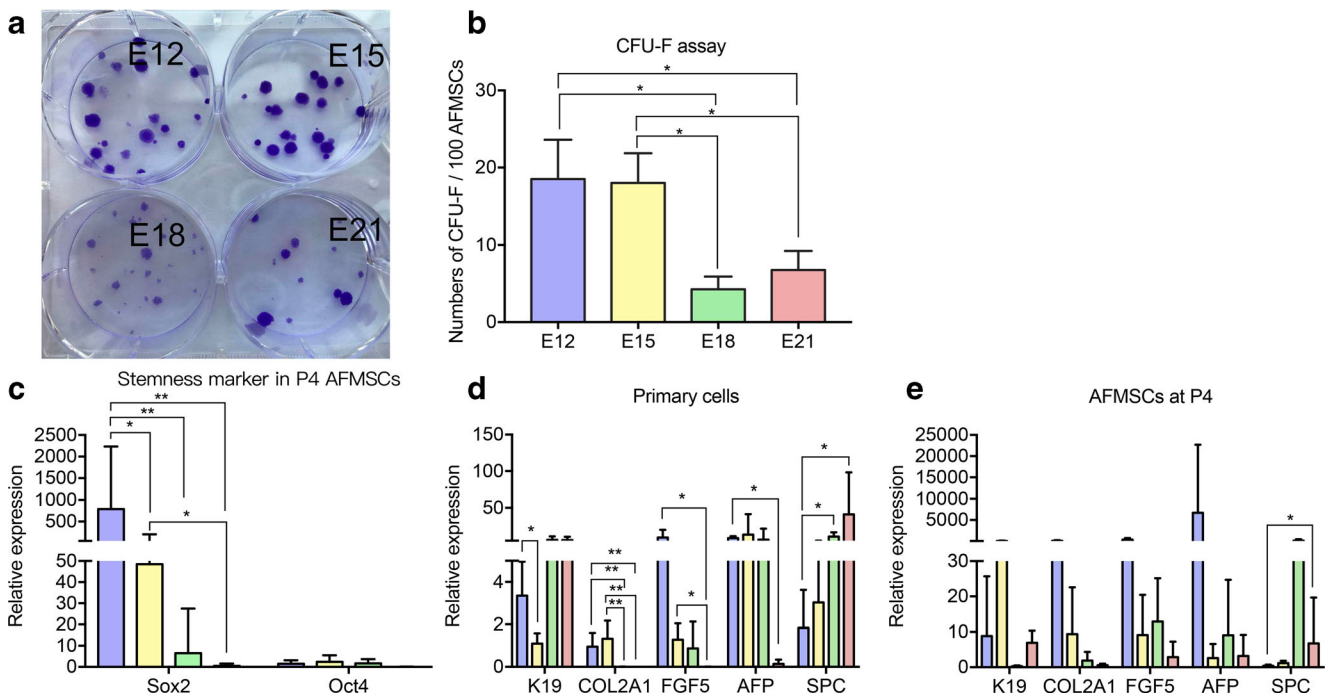


**Figure 5.** CFU-F assay and gene expression levels of the rat AFMSCs derived from four gestational stages. (a) CFU-F assay of the four groups of AFMSCs at P5 stained with crystal violet staining solution. (b) The CFU-F number was microscopically scored by counting colonies ( $\geq 50$  cells) with clear spindle-shaped fibroblast-like morphology and excluding colonies with round epithelioid-like morphology. Four replicate samples were used in the CFU-F assay. (c) Expression levels of the pluripotent

stem cell markers Sox2 ( $n = 6$ ) and Oct4 ( $n = 3$ ) detected using RT-qPCR. Sox2 expression was significantly higher in E12 and E15 cells than in E18 and E21 cells. (d) Expression levels of K19, Col2A1, FGF5, AFP, and SPC in primary cells derived from the four stages of pregnancy ( $n = 3$ ). (e) Expression levels of K19, Col2A1, FGF5, AFP, and SPC in AFMSCs at P4.  $n = 3$ ,  $*p < 0.05$ ;  $**p < 0.01$ .

is a marker of pluripotency and the Sox2/Oct4 complex is at the top of the pluripotent regulatory hierarchy (Rodda *et al.* 2005). Thus, a change in either gene can affect pluripotency. In addition, Nanog expression was not observed at any cell stage. Nanog does not affect the self-renewal potential of stem cells (Cavaleri and Scholer 2003). Fernandes *et al.* (2012) showed that Nanog was not expressed in canine full-term AF stem cells. Their finding is consistent with our experiments and might explain why the established AFMSC populations from E12 and E15 could be easily maintained for more than 60 passages without growth slowing, compared with only 10 passages for the cells derived from E18 and E21.

The expression profiles of K19, Col2A1, FGF5, AFP, and SPC were also identified. The results indicated mixed populations of AFMSCs co-existed in the AFMSC cultures, particularly AFMSCs derived from E12 and E15 AF. At E12, the AFMSCs were derived from all three germ layers and fetal skin because the primary AF cells at E12 as well as the E12 AFMSCs expressed the markers of all three germ layers and skin (Esteves *et al.* 2017). Similarly, the E15 AFMSCs were derived from the mesoderm, ectoderm, and fetal skin, the E18 AFMSCs mainly came from the three germ layers and respiratory tract, and the E21 AFMSCs were derived

from the mesoderm, ectoderm, and fetal skin. These findings may be associated with the embryonic developmental process. At the early stage of embryo development (E12), three germ layers have formed. Thus, the AFMSCs from E12 mainly express the markers of three germ layers. Then, the germ layers begin to differentiate, with differentiation first occurring in the ectoderm and then the endoderm. In addition, the dermis begins to form (Hill 2019). This leads to increased K19 expression which is why E15 AFMSCs mainly express the mesoderm, ectoderm, and fetal skin markers. At the late stage of embryo development (E18 and E21), because all the organs have formed and the fetal tissue is fully grown, more markers could be observed, and due to the appearance of extensive airway branching and the exchange of lung fluid (Hill 2019), E18 and E21 AFMSCs express markers of the skin, three germ layers, and respiratory tract. In addition, in the early stage of embryonic development, mesenchymal cells cluster first and then differentiate into chondrocytes, with cartilage gradually replaced by bone tissue (Pines and Hurwitz 1991). Because the clustering process occurs at the early stage of embryonic development, the early AF likely contained mesenchymal cells that expressed the chondrocyte

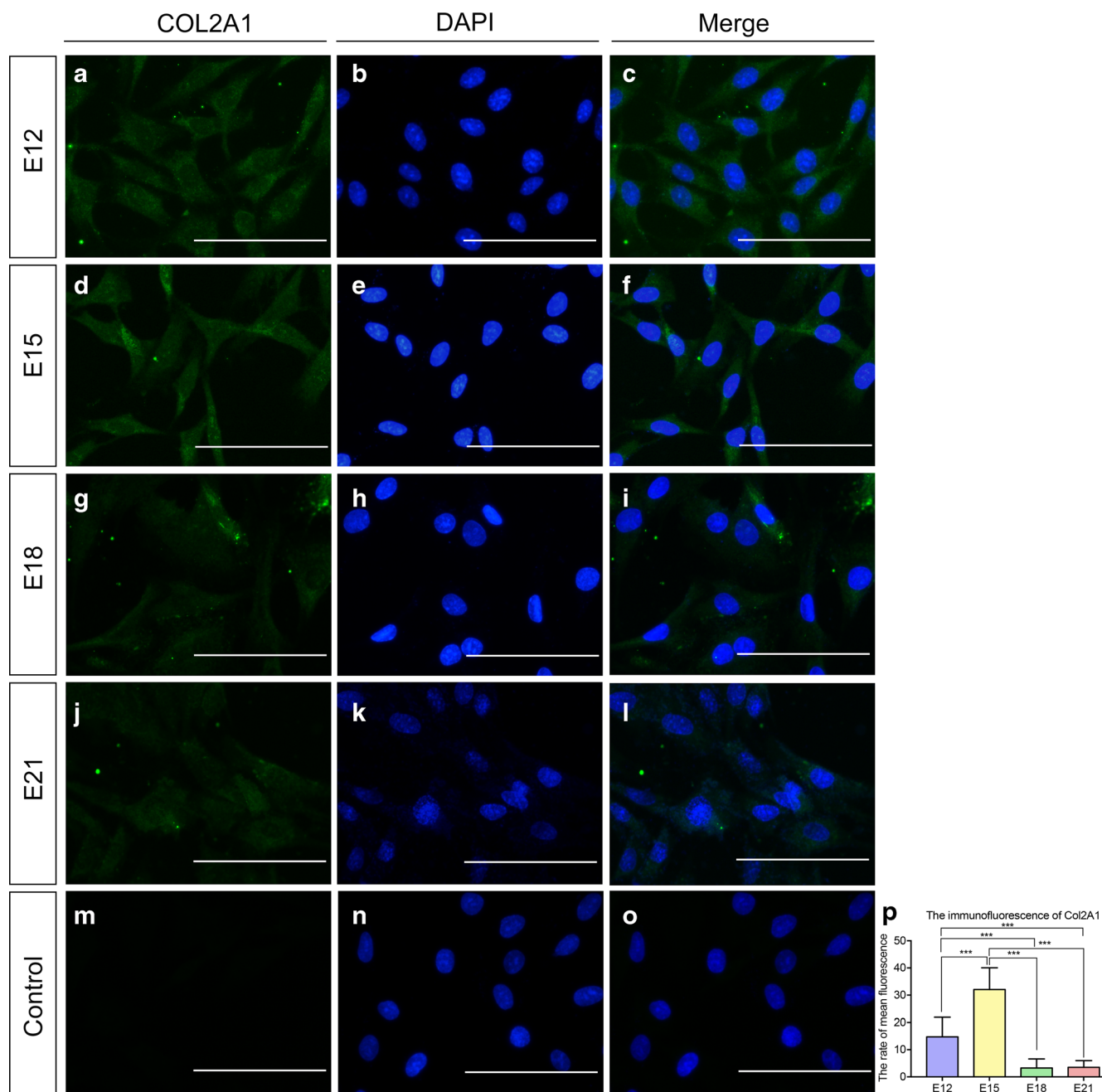


**Figure 6.** Immunofluorescence of COL2A1 in AFMSCs derived from four different gestational stages. (a–c) The COL2A1 expression in E12 AFMSCs. (d–f) The COL2A1 expression in E15 AFMSCs. (g–i) The COL2A1 expression in E18 AFMSCs. (j–l) The COL2A1 expression in

E21 AFMSCs. (m–o) Negative control of immunofluorescence stained with anti-rabbit IgG (Alexa Fluor® 488 Conjugate). Scale bar = 50  $\mu\text{m}$ ,  $n = 3$ . (p) The statistical histogram of COL2A1 mean immunofluorescence rate; Kruskal-Wallis test, chi-squared = 30.64,  $n = 10$ ,  $***p < 0.001$ .

marker. The later trimester did not have the mesenchymal cell clustering process thus did not show significant COL2A1 expression. Therefore, the AFMSCs expressing COL2A1 probably originated from the embryonic mesoderm, which is consistent with the source of the bone marrow MSCs discussed above. Thus, in this study, we have identified the MSCs derived from the different stages of the pregnant rats and have shown that they possess altered proliferation and differentiation potential

which in turn gives a new insight into their potential clinical applications. As the “self-renewal” capability of a stem cell can be determined at a single-cell level and regulated throughout its life span in response to intrinsic signals, like transcriptional factors (Liu *et al.* 2016), and external circumstances, like the amniotic fluid at the different stages, it would be interesting to compare not only the “self-renewal” capabilities of the MSCs between different stages of pregnancy, but also the different types of

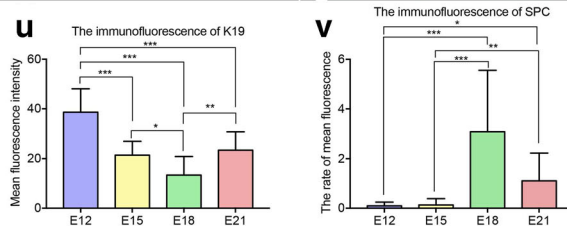
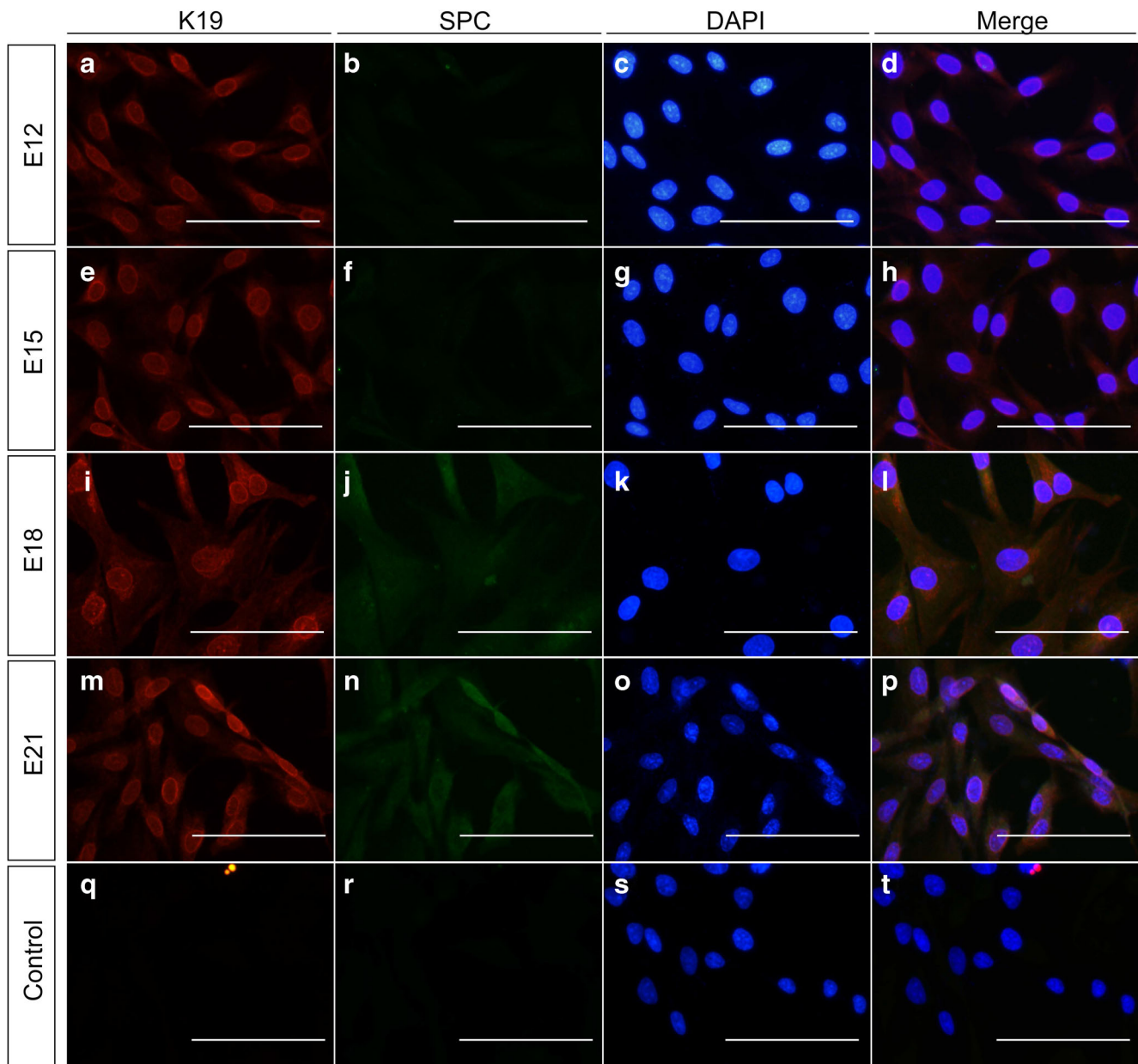


**Figure 7.** Double immunofluorescence staining of K19 and SPC in AFMSCs derived from four different gestational stages. (*a–d*) The double immunofluorescence staining of E12 AFMSCs. (*a*) The K19 expression (*red*). (*b*) The SPC expression (*green*). The SPC expression is barely detected. (*e–h*) The double immunofluorescence staining of E15 AFMSCs. (*e*) The K19 expression (*red*). (*f*) The SPC expression (*green*). The SPC expression also was barely detected. (*i–l*) The double immunofluorescence staining of E18 AFMSCs. (*i*) The K19 expression (*red*). (*j*) The SPC expression (*green*). The SPC expression in E18 AFMSCs was significantly higher than in E12 and E15 AFMSCs. (*m–p*) The double immunofluorescence staining of E21 AFMSCs. (*m*) The

K19 expression (*red*). (*n*) The SPC expression (*green*). The SPC expression was similar to the expression in E18 AFMSCs and significantly higher than in E12 and E15 AFMSCs. (*q–t*) Negative control of immunofluorescence. (*q*) Staining with anti-mouse IgG (Alexa Fluor® 555 Conjugate). (*r*) Staining with anti-rabbit IgG (Alexa Fluor® 488 Conjugate). Scale bar = 50  $\mu$ m,  $n = 3$ . (*u*) The statistical histogram of K19 mean immunofluorescence rate; ANOVA, F value = 19.291,  $n = 10$ . (*v*) The statistical histogram of SPC mean immunofluorescence rate; Kruskal-Wallis test, chi-squared = 25.251,  $n = 10$ , \* $p < 0.05$ ; \*\* $p < 0.01$ ; \*\*\* $p < 0.001$ .

MSCs from the heterogeneous populations at the same stages of pregnancy and during their life spans.

## Conclusion

In the present study, the AFMSC populations derived from four stages of AF cells of pregnant rats were isolated and investigated. The cells derived from E15 AF were the smallest in size and easiest to culture, displayed a higher stemness potential, and could be passaged more than 60 times while still maintaining a proliferative state; however, the E18 and E21 cells could only be cultured for 10 passages. The AFMSCs derived from E15 had higher viabilities and proliferative capacity than cells from the late stages. AF cells from early stages could be good candidates to explore potential treatments involving AFMSCs. In addition, the expression levels of the K19, Col2A1, FGF5, AFP, and SPC genes indicate mixed-population cells co-exist in the AFMSC cultures.

**Funding** This work was supported by the National Natural Science Foundation of China (Grant numbers: 81871219, 81671469, 81901565) and the National Key Research and Development Program (2016YFC1000505).

## References

- Akagi T, Kuure S, Uranishi K, Koide H, Costantini F, Yokota T (2015) ETS-related transcription factors ETV4 and ETV5 are involved in proliferation and induction of differentiation-associated genes in embryonic stem (ES) cells. *J Biol Chem* 290:22460–22473
- Alessio N, Pipino C, Mandatori D, Di Tomo P, Ferone A, Marchiso M, Melone MAB, Peluso G, Pandolfi A, Galderisi U (2018) Mesenchymal stromal cells from amniotic fluid are less prone to senescence compared to those obtained from bone marrow: an in vitro study. *J Cell Physiol* 233:8996–9006
- Billing AM, Ben Hamidane H, Dib SS, Cotton RJ, Bhagwat AM, Kumar P, Hayat S, Yousri NA, Goswami N, Suhre K, Rafii A, Graumann J (2016) Comprehensive transcriptomic and proteomic characterization of human mesenchymal stem cells reveals source specific cellular markers. *Sci Rep* 6:21507
- Caplan AI (1991) Mesenchymal stem cells. *J Orthop Res* 9:641–650
- Cavaleri F, Scholer HR (2003) Nanog: a new recruit to the embryonic stem cell orchestra. *Cell* 113:551–557
- Chen W, Siegel N, Li L, Pollak A, Hengstschlager M, Lubec G (2009) Variations of protein levels in human amniotic fluid stem cells CD117/2 over passages 5–25. *J Proteome Res* 8:5285–5295
- De Coppi P, Bartsch G Jr, Siddiqui MM, Xu T, Santos CC, Perin L, Mostoslavsky G, Serre AC, Snyder EY, Yoo JJ, Furth ME, Soker S, Atala A (2007) Isolation of amniotic stem cell lines with potential for therapy. *Nat Biotechnol* 25:100–106
- Dominici M, Le Blanc K, Mueller I, Slaper-Cortenbach I, Marini F, Krause D, Deans R, Keating A, Prockop D, Horwitz E (2006) Minimal criteria for defining multipotent mesenchymal stromal cells. The International Society for Cellular Therapy position statement. *Cytotherapy* 8:315–317
- Dostert G, Mesure B, Menu P, Velot E (2017) How do mesenchymal stem cells influence or are influenced by microenvironment through extracellular vesicles communication? *Front Cell Dev Biol* 5:6
- Esteves CL, Sheldrake TA, Dawson L, Menghini T, Rink BE, Amilon K, Khan N, Peault B, Donadeu FX (2017) Equine mesenchymal stromal cells retain a pericyte-like phenotype. *Stem Cells Dev* 26:964–972
- Fernandes RA, Wenceslau CV, Reginato AL, Kerkis I, Miglino MA (2012) Derivation and characterization of progenitor stem cells from canine allantois and amniotic fluids at the third trimester of gestation. *Placenta*. 33:640–644
- Friedenstein AJ (1976) Precursor cells of mechanocytes. *Int Rev Cytol* 47:327–359
- Galipeau J, Sensebe L (2018) Mesenchymal stromal cells: clinical challenges and therapeutic opportunities. *Cell Stem Cell* 22:824–833
- Harrell CR, Gazdic M, Fellabaum C, Jovicic N, Djonov V, Arsenijevic N, Volarevic V (2019) Therapeutic potential of amniotic fluid derived mesenchymal stem cells based on their differentiation capacity and immunomodulatory properties. *Curr Stem Cell Res Ther* 14:327–336
- Hill MA (2019) Embryology rat development. [https://embryology.med.unsw.edu.au/embryology/index.php/Rat\\_Development](https://embryology.med.unsw.edu.au/embryology/index.php/Rat_Development). Accessed 19 Jan 2019
- Hoepfner J, Kleinsorge M, Papp O, Ackermann M, Alfken S, Rinas U, Solodenko W, Kirschning A, Sgodda M, Cantz T (2016) Biphasic modulation of Wnt signaling supports efficient foregut endoderm formation from human pluripotent stem cells. *Cell Biol Int* 40:534–548
- Honarpardaz A, Irani S, Pezeshki-Modaress M, Zandi M, Sadeghi A (2019) Enhanced chondrogenic differentiation of bone marrow mesenchymal stem cells on gelatin/glycosaminoglycan electrospun nanofibers with different amount of glycosaminoglycan. *J Biomed Mater Res A* 107:38–48
- Irfan-Maqsood M, Matin MM, Heirani-Tabasi A, Bahrami M, Naderi-Meshkin H, Mirahmadi M, Hassanzadeh H, Sanjar Moussavi N, Raza-Shah H, Raeesolmohaddeseen M, Bidkhorji H, B. AR. (2016) Adipose derived mesenchymal stem cells express keratinocyte lineage markers in a co-culture model. *Cell Mol Biol (Noisy-le-grand)* 62:44–54
- Jensen TJ, Shui JE, Finck CM (2017) The effect of meconium exposure on the expression and differentiation of amniotic fluid mesenchymal stem cells. *J Neonatal-Perinatal Med* 10:313–323
- Kaviani A, Perry TE, Dzakovic A, Jennings RW, Ziegler MM, Fauza DO (2001) The amniotic fluid as a source of cells for fetal tissue engineering. *J Pediatr Surg* 36:1662–1665
- Lesage F, Pranpanus S, Bosisio FM, Jacobs M, Ospitalieri S, Toelen J, Deprest J (2017) Minimal modulation of the host immune response to SIS matrix implants by mesenchymal stem cells from the amniotic fluid. *Hemia*. 21:973–982
- Li Y, Gu C, Xu W, Yan J, Xia Y, Ma Y, Chen C, He X, Tao H (2014) Therapeutic effects of amniotic fluid-derived mesenchymal stromal cells on lung injury in rats with emphysema. *Respir Res* 15:120
- Liu TM, Lee EH, Lim B, Shyh-Chang N (2016) Concise review: balancing stem cell self-renewal and differentiation with PLZF. *Stem Cells* 34:277–287
- Moschidou D, Mukherjee S, Blundell MP, Drews K, Jones GN, Abdulrazzak H, Nowakowska B, Phoolchand A, Lay K, Ramasamy TS, Cananzi M, Nettersheim D, Sullivan M, Frost J, Moore G, Vermeesch JR, Fisk NM, Thrasher AJ, Atala A, Adjaye J, Schorle H, De Coppi P, Guillot PV (2012) Valproic acid confers functional pluripotency to human amniotic fluid stem cells in a transgene-free approach. *Mol Ther* 20:1953–1967
- Mun-Fun H, Ferdaos N, Hamzah SN, Ridzuan N, Hisham NA, Abdullah S, Ramasamy R, Cheah PS, Thilakavathy K, Yazid MN, Nordin N (2015) Rat full term amniotic fluid harbors highly potent stem cells. *Res Vet Sci* 102:89–99
- Pines M, Hurwitz S (1991) The role of the growth plate in longitudinal bone growth. *Poult Sci* 70:1806–1814

- Pratheesh MD, Gade NE, Katiyar AN, Dubey PK, Sharma B, Saikumar G, Amaral, Sharma GT (2013) Isolation, culture and characterization of caprine mesenchymal stem cells derived from amniotic fluid. *Res Vet Sci* 94:313–319
- Rahman MS, Spitzhorn LS, Wruck W, Hagenbeck C, Balan P, Graffmann N, Bohndorf M, Ncube A, Guillot PV, Fehm T, Adjaye J (2018) The presence of human mesenchymal stem cells of renal origin in amniotic fluid increases with gestational time. *Stem Cell Res Ther* 9:113
- Rodda DJ, Chew JL, Lim LH, Loh YH, Wang B, Ng HH, Robson P (2005) Transcriptional regulation of nanog by OCT4 and SOX2. *J Biol Chem* 280:24731–24737
- Rossi B, Merlo B, Colleoni S, Iacono E, Tazzari PL, Ricci F, Lazzari G, Galli C (2014) Isolation and in vitro characterization of bovine amniotic fluid derived stem cells at different trimesters of pregnancy. *Stem Cell Rev* 10:712–724
- Roubelakis MG, Bitsika V, Zagoura D, Trohatou O, Pappa KI, Makridakis M, Antsaklis A, Vlahou A, Anagnou NP (2011) In vitro and in vivo properties of distinct populations of amniotic fluid mesenchymal progenitor cells. *J Cell Mol Med* 15:1896–1913
- Samsonraj RM, Rai B, Sathyanathan P, Puan KJ, Röttschke O, Hui JH, Raghunath M, Stanton LW, Nurcombe V, Cool SM (2015) Establishing criteria for human mesenchymal stem cell potency. *Stem Cells* 33:1878–1891
- Savickiene J, Treigyte G, Baronaite S, Valiulienė G, Kaupinis A, Valius M, Arlauskienė A, Navakauskienė R (2015) Human amniotic fluid mesenchymal stem cells from second- and third-trimester amniocentesis: differentiation potential, molecular signature, and proteome Analysis. *Stem Cells Int* 2015:1–15
- Savickienė J, Baronaite S, Zentelytė A, Treigyte G, Navakauskienė R (2016) Senescence-associated molecular and epigenetic alterations in mesenchymal stem cell cultures from amniotic fluid of normal and fetus-affected pregnancy. *Stem Cells Int* 2016:1–13
- Schiavo AA, Franzin C, Albiero M, Piccoli M, Spiro G, Bertin E, Urbani L, Visentin S, Cosmi E, Fadini GP, De Coppi P, Pozzobon M (2015) Endothelial properties of third-trimester amniotic fluid stem cells cultured in hypoxia. *Stem Cells Ther* 6:209
- Spitzhorn LS, Rahman MS, Schwindt L, Ho HT, Wruck W, Bohndorf M, Wehrmeyer S, Ncube A, Beyer I, Hagenbeck C, Balan P, Fehm T, Adjaye J (2017) Isolation and molecular characterization of amniotic fluid-derived mesenchymal stem cells obtained from caesarean sections. *Stem Cells Int* 2017:5932706
- Underwood MA, Gilbert WM, Sherman MP (2005) Amniotic fluid: not just fetal urine anymore. *J Perinatol* 25:341–348
- Zheng Y, Gao Z, Xie C, Zhu H, Peng L, Chen J, Chong Y (2008) Characterization and hepatogenic differentiation of mesenchymal stem cells from human amniotic fluid and human bone marrow: a comparative study. *Cell Biol Int* 32:1439–1448